

# p-Pb collisions at 5.02 TeV in the Parton-Hadron-String-Dynamics transport approach

V P Konchakovski<sup>1</sup>, W Cassing<sup>1</sup> and V D Toneev<sup>2</sup>

<sup>1</sup> Institute for Theoretical Physics, University of Giessen, 35392 Giessen, Germany

<sup>2</sup> Joint Institute for Nuclear Research, 141980 Dubna, Russia

**Abstract.** The Parton-Hadron-String-Dynamics (PHSD) transport model is employed for p-Pb collisions at  $\sqrt{s_{NN}} = 5.02$  TeV and compared to recent experimental data from the LHC as well as to alternative models. We focus on the question of initial state dynamics, i.e. if the initial state might be approximated by a superposition of independent nucleon-nucleon collisions or should be considered as a coherent gluon field as predicted within the color glass condensate (CGC) framework. We find that the PHSD approach provides correlations between the charged particle multiplicity at midrapidity and the number of participant nucleons close to results from the CGC and differs substantially from results calculated with independent Glauber initial conditions. However, a sizeable difference is found between the PHSD approach and CGC models with respect to the rapidity dependence of the average transverse momentum. Accordingly, related measurements at LHC should allow to prove or disprove the presence of coherent colour fields in the initial phase of the collisions.

PACS numbers: 25.75.-q, 24.85.+p, 12.38.Mh

Submitted to: *J. Phys. G: Nucl. Phys.*

## 1. Introduction

Ultra-relativistic nucleus-nucleus collisions provide an opportunity for exploring strongly interacting QCD matter under extreme conditions which is the ultimate goal of heavy-ion experiments at the relativistic heavy-ion collider (RHIC) and the large hadron collider (LHC). The experiments at the RHIC and the LHC have demonstrated that a stage of partonic matter is produced in these reactions which is in an approximate equilibrium for a few fm/c [1, 2]. Due to the non-perturbative and non-equilibrium nature of relativistic nuclear reaction systems, their theoretical description is based essentially on a variety of effective models ranging from hydrodynamic models with different initial conditions [3, 4, 5, 6, 7, 8, 9, 10, 11, 12] to various kinetic approaches [13, 14, 15, 16, 17, 18, 19] or different types of hybrid models [20, 21, 22, 23, 24, 25, 26] that employ conceptually different assumptions on the initial conditions. In the latter approaches the initial state models are followed by an ideal or viscous hydro phase which after freeze-out is completed by a hadronic cascade simulation. However, a commonly accepted and complete picture is still lacking and precise data from the RHIC and LHC are expected to clarify the situation. The actual questions addressed in this study are whether the initial state of the colliding nuclei behaves like a superposition of its constituents or as a coherent gluon field as predicted in the color glass condensate (CGC) framework [27]. Furthermore, we address the problem of how to disentangle the different initial state scenarios in final state observables.

The different phenomenological models that successfully describe heavy-ion data include coherence effects in the initial state which can be identified at the level of the wave function and also at the level of primary particle production. A complete, QCD-based, dynamical description of the coherence effects is provided within the color glass condensate concept (cf. the reviews [27]). Here, gluon shadowing is taken into account through nonlinear renormalization group equations, i.e. the BK-JIMWLK evolution of classical Yang-Mills equations that describe gluon fusion at soft momentum scales. They imply the emergence of a dynamical transverse momentum scale, the saturation scale  $Q_s$ , such that gluon modes with transverse momentum  $k_t \leq Q_s(x)$  are in the saturation regime [27]. Such a saturation/suppression of gluon densities is equivalent to the presence of strong coherent color fields. Unfortunately, there is no direct experimental observable that proves the existence of such coherent color fields (or CGC). To validate the CGC approach, one should compare different observables calculated within CGC models with alternative approaches that do not involve the concept of coherent color fields.

Conventional descriptions of ultrarelativistic heavy-ion reactions are ideal or viscous hydrodynamic models [3, 4, 5, 6, 7, 8, 9, 10, 11, 12] or hybrid approaches [20, 21, 22, 23, 24, 25, 26] which can be examined also on an event-by-event basis [28, 29]. In these hydro calculations the initial conditions – at some finite starting time of the order of 0.5 fm/c – have to be evaluated either in terms of the (standard) Glauber model or other initial state scenarios like in the IP-glasma model [28] or the CGC approach,

respectively. Differences between the different initial state assumptions and dynamical evolutions thus have to be expected. The applicability of ideal or viscous hydrodynamic models to proton-nucleus reactions for low multiplicity events, however, is very much debated. This also holds for hybrid models as long as they employ a hydro phase.

The flow harmonics  $v_n$  have been found to be sensitive to the early stage of nuclear interaction and in particular their fluctuations. Indeed, the detailed heavy-ion analysis in Ref. [30] shows that Monte Carlo CGC approaches (MC-CGC) systematically give a larger initial eccentricity than Glauber models. However, it is unclear to what extent such properties of the CGC formalism are robust with respect to extended correlations. Also, studies of higher harmonics – as presented in [2] by the PHENIX or ALICE collaborations – do not clearly favor the CGC or Glauber assumptions for the initial state of the collision. The first LHC data on the bulk particle production in Pb-Pb collisions are in good agreement with improved CGC expectations but they are also compatible with Monte Carlo event generators [1, 31]. Both models have in common that they include some ‘coherence effects’.

The complexity of heavy-ion collisions is reduced essentially in the case of proton-nucleus collisions owing to the expected dominance of the initial state effects. Recently, the first preliminary ALICE measurement of the charged particle pseudorapidity density has been reported [32] for  $|\eta| < 2$  in p-Pb collisions at a nucleon-nucleon center-of-mass energy  $\sqrt{s_{NN}} = 5.02$  TeV. The measurement is compared to two sets of particle production models that describe similar measurements for other collision systems: the saturation models employing coherence effects [33, 34, 35] and the two-component models combining perturbative QCD processes with soft interactions [36, 37]. A comparison of the model calculations with the data shows that the results are model-dependent and predict the measured multiplicity values only within 20%. Accordingly, the restrictions imposed by the measured minimal bias pseudorapidity spectra  $dN_c/d\eta$  are not sufficient to disentangle different models for the very early interaction stage of ultrarelativistic collisions. A large set of various characteristic predicted in the compilation [38] for p-Pb collisions at 5.02 TeV is still waiting for a proper analysis/comparison.

A test of color coherence in proton-nucleus collisions at the LHC energy has been proposed in Ref. [39]. The idea of this proposal is based on the fact that the observed mean multiplicity of charged particles  $\langle N_{ch} \rangle$  linearly depends on the number of participants  $N_{part}$  within the wounded nucleon model (WNM) of independent nucleon-nucleon scatterings,  $\langle N_{ch} \rangle \sim N_{part}$ , while in the CGC models this dependence is logarithmic,  $\langle N_{ch} \rangle \sim \ln N_{part}$ . For a small number of participants,  $N_{part} \leq 10$ , the mean multiplicities calculated in both approaches practically coincide (in agreement with experiment) but for  $N_{part} \sim 25$  they differ by almost a factor of two [39]. Such large numbers of participant are possible at the LHC energy of 5.02 TeV in p-Pb collisions. Furthermore, as pointed out in Ref. [40] there should be a sizeable difference in the mean transverse momentum of particles versus the pseudorapidity  $\langle p_T \rangle(\eta)$  with opposite slopes in  $\eta$  on the projectile side within the CGC framework relative to hydrodynamical

calculations due the saturation scale  $Q_s$  in the CGC.

Following these suggestions we here study the charged particle multiplicities and related quantities in p-Pb interactions at the collision energy  $\sqrt{s_{NN}} = 5.02$  TeV within the parton-hadron-string-dynamics (PHSD) transport approach [19] which has been properly upgraded to LHC energies with respect to a more recent PYTHIA implementation (Sec. II). Predictions for various observables and their correlations are given in Sec. III which are also compared to available data as well as to results from CGC saturation models. We conclude our findings in Sec. IV.

## 2. PHSD @ LHC

The PHSD model is a covariant dynamical approach for strongly interacting systems formulated on the basis of Kadanoff-Baym equations [41] or off-shell transport equations in phase-space representation, respectively. In the Kadanoff-Baym theory the field quanta are described in terms of dressed propagators with complex selfenergies. Whereas the real part of the selfenergies can be related to mean-field potentials (of Lorentz scalar, vector or tensor type), the imaginary parts provide information about the lifetime and/or reaction rates of time-like particles [42]. Once the proper (complex) selfenergies of the degrees of freedom are known, the time evolution of the system is fully governed by off-shell transport equations (as described in Refs. [41, 42]). This approach allows for a simple and transparent interpretation of lattice QCD results for thermodynamic quantities as well as correlators and leads to effective strongly interacting partonic quasiparticles with broad spectral functions. For a review on off-shell transport theory we refer the reader to Ref. [42]; model results and their comparison with experimental observables for heavy-ion collisions from the lower super-proton-synchrotron (SPS) to RHIC energies can be found in Refs. [19, 43, 44] including electromagnetic probes such as  $e^+e^-$  or  $\mu^+\mu^-$  pairs [45]. We mention that the PHSD model takes into account some kind of 'coherent effects' with respect to QCD showers since it includes corrections to the leading-log picture – denoted as coherence effects – that lead to an ordering of subsequent emissions in terms of decreasing angles.

To extend the PHSD model to higher energies than  $\sqrt{s_{NN}} = 200$  GeV at RHIC, we have additionally implemented the PYTHIA 6.4 generator [46] for initial nucleon collisions at LHC energies. For the subsequent (lower energy) collisions the standard PHSD model [19] is applied (including PYTHIA v5.5 with JETSET v7.3 for the production and fragmentation of jets [47], i.e. for  $\sqrt{s_{NN}} \leq 500$  GeV [47]). In this way all results from PHSD up to top RHIC energies are regained and a proper extension to LHC energies is achieved. At  $\sim \sqrt{s_{NN}} = 500$  GeV both PYTHIA versions lead to very similar results. In PYTHIA 6.4 we use the Innsbruck pp tune (390) which allows to describe reasonably the p-p collisions at  $\sqrt{s_{NN}} = 7$  TeV in the framework of the PHSD transport approach (cf. Fig. 1). Here the overall agreement with LHC experimental data for the distribution in the charged particle multiplicity  $N_{ch}$  (a), the charged particle pseudorapidity distribution (b), the transverse momentum  $p_T$

spectra (c) and the correlation of the average  $p_T$  with the number of charged particles (d) is satisfactory. One should note that the experimental results of different LHC collaborations slightly differ (within errorbars). In particular, the pseudorapidity and transverse momentum distributions of the CMS Collaboration are slightly below those of the ATLAS Collaboration. In addition, different PYTHIA tunes, being generally in satisfactory agreement with pp data and tuned to specific observables, describe the tails of  $N_{ch}$  and  $p_T$  distributions with different quality.

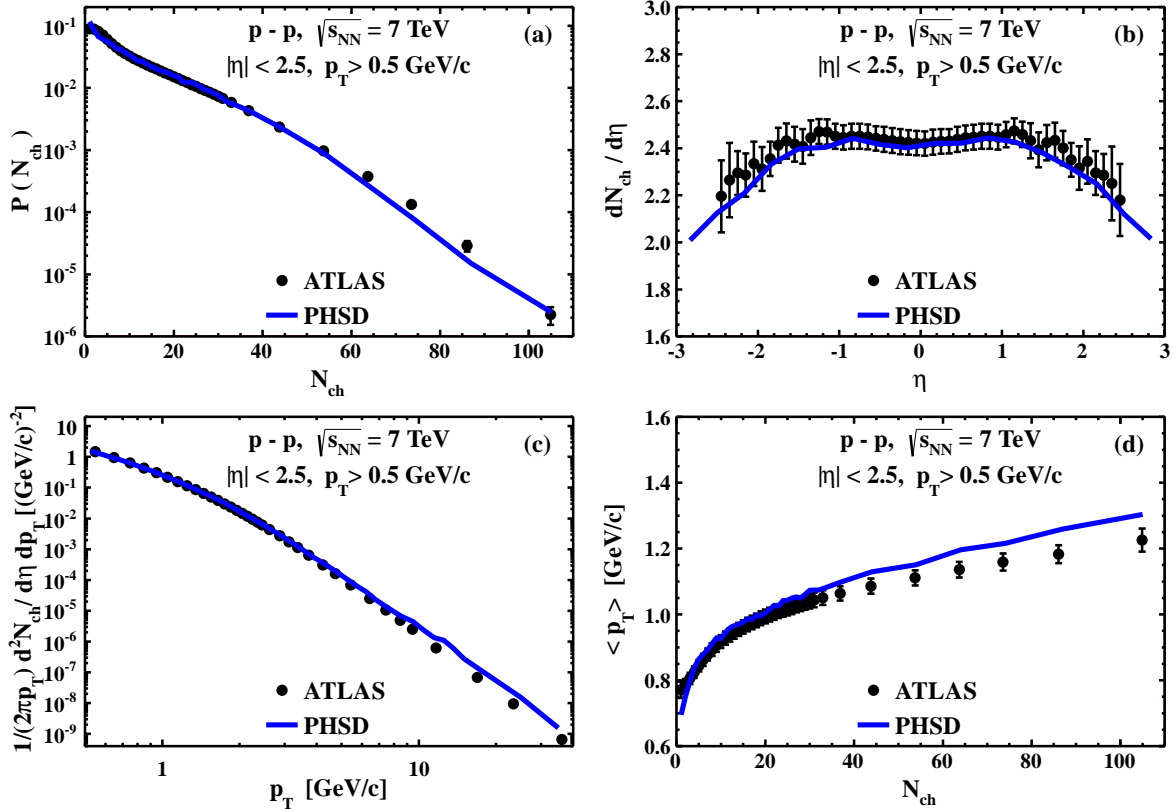


**Figure 1.** Comparison of the PHSD results (including PYTHIA 6.4) with LHC experimental data from the ATLAS Collaboration [48] for p-p collisions at  $\sqrt{s_{NN}} = 7$  TeV: (a)  $N_{ch}$  distribution, (b)  $dN_{ch}/d\eta$  distribution, (c)  $p_T$ -spectra and (d) average  $p_T$  vs.  $N_{ch}$ .

Although PYTHIA 6.4 includes some elements of coherence in the creation of particles (by string fusion, string fragmentation, quasiparticle spectral densities etc.) it deviates substantially from the early interaction stage in the CGC approach [27]. We mention that initial state fluctuations in hydro calculations are usually imposed by independent Glauber model simulations or MC-KLN initial conditions [49], respectively. Initial conditions very similar to the Glauber model are included by default in the PHSD transport approach, however, with an essential difference: the energy-momentum conservation is fulfilled exactly in every collision such that the entire dynamics conserves four-momentum as well as all discrete conservation laws. We recall that the PHSD approach has been tested successfully for collective flows  $v_1, v_2, v_3$  and  $v_4$  in nucleus-

nucleus collisions from lower super-proton-synchrotron (SPS) up to RHIC energies [43] where especially the uneven flow coefficients are sensitive to the initial state fluctuations. Accordingly, the initial fluctuations in energy density - in the transverse plane - from PHSD are in accord with experimental observation.

It has been argued, furthermore, that in high energy p-A collisions the Glauber model should be corrected/extended to account for the fact that between successive interactions the incoming proton is off-shell [50] and may fluctuate in size. In addition, event-to-event fluctuations in the configuration of the incoming proton can change its effective scattering cross section as noted in Refs. [51, 52, 53]. The concept of hadronic cross-section fluctuations incorporates the physics of color transparency and color opacity into the dynamics of relativistic nuclear collisions. In order to evaluate the impact of these fluctuations of the projectile proton, a modified version of the Glauber Monte Carlo, referred to as 'Glauber-Gribov' MC, is implemented additionally/optionally in the PHSD. Following Refs. [51, 52, 53], the probability distribution in the total cross sections  $\sigma_{tot}$  is taken to be

$$P_h(\sigma_{tot}) = a_h \frac{\sigma_{tot}}{\sigma_{tot} + \sigma_0} \exp \left( -\frac{(\sigma_{tot}/\sigma_0 - 1)^2}{\Omega^2} \right). \quad (1)$$

Here,  $a_h$  is a normalization constant,  $\Omega$  controls the width of the  $P_h(\sigma_{tot})$  distribution, and  $\sigma_0$  determines  $\langle \sigma_{tot}(\sqrt{s}) \rangle$  which is adopted from PYTHIA 6.4. Estimates of  $\Omega$  have been provided in Ref. [53] for center-of-mass energies of 1.8, 9, and 14 TeV. We use two interpolations of these values that for  $\sqrt{s_{NN}} = 5.02$  TeV results in  $\Omega = 0.55$  or, in accordance with the recent analysis in Ref. [53], to  $\Omega = 1.01$  which enhances the influence of fluctuations. The elastic fraction of the total cross-section in (1) is taken to be constant [53],  $\sigma_{NN} = \lambda \sigma_{tot}$  (following [53]  $\lambda$  is weakly changing with energy and the actual value employed is  $\lambda = 0.26$ ); the probability distribution for  $\sigma_{NN}$  then is given by  $P_H(\sigma_{NN}) = (1/\lambda)P(\sigma_{NN}/\lambda)$ . The actual values for the elastic and inelastic cross sections in PHSD are determined by Monte Carlo according to the distribution (1).

### 3. Properties of p-Pb collisions

#### 3.1. Energy density in a single p-Pb event

The energy density  $\epsilon$  in local cells from PHSD is presented in Fig. 2 in the transverse ( $x - y$ ) plane (a) as well as the reaction ( $x - z$ ) plane (b) for a single p-Pb event at  $\sqrt{s_{NN}} = 5.02$  TeV. Here we have selected an event that leads to about 300 charged hadrons in the final state. The time of this event ( $t = 0.002$  fm/c) corresponds to the moment when the proton has passed the Lorentz contracted nucleus and is very small compared to the initial times considered for hydrodynamical models ( $\sim 0.5 - 1$  fm/c). Note that the energy density at this moment is huge due to the fact that the spacial volume is very tiny ( $\sim 5 \cdot 10^{-3}$  fm<sup>3</sup>) and the full inelasticity of the previous inelastic reactions is incorporated. Due to the Heisenberg uncertainty relation this energy density cannot be specified as being due to 'particles' since the latter may form only much later

on a timescale of their inverse transverse mass (in their rest frame). More specifically, only a jet at midrapidity with transverse momentum  $p_T = 100$  GeV is expected to appear at  $t \approx 2 \cdot 10^{-3}$  fm/c while a soft parton with transverse momentum  $p_T = 0.5$  GeV should be formed after  $t \approx 0.4$  fm/c). At this time the energy density  $\epsilon$  is lower by more than a factor of 200 due to the dominant longitudinal expansion.

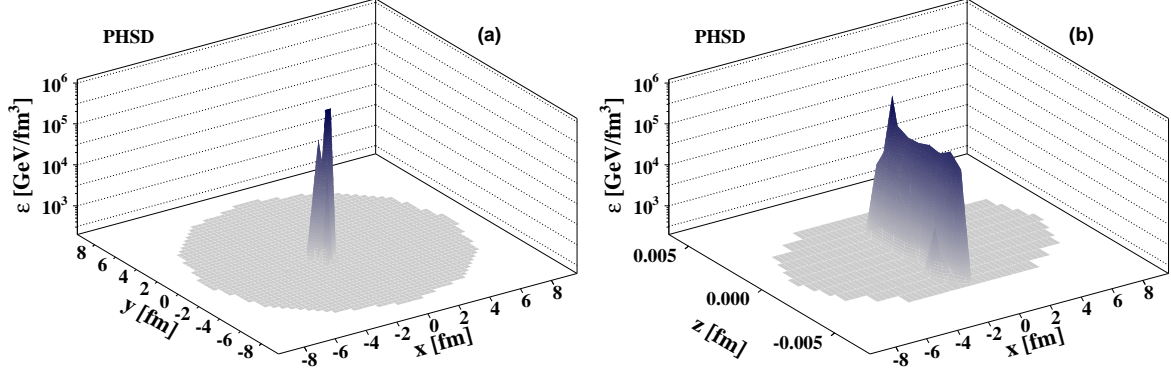


**Figure 2.**  $x-y$  (a) and  $x-z$  (b) projections of the energy density in a single (highly inelastic) p-Pb event ( $\sqrt{s_{NN}} = 5.02$  TeV) at the time when the proton-remnant has passed through the Pb-nucleus ( $t = 0.002$  fm/c). The region occupied by the Pb nucleus is also shown by the shaded area. Note the Lorentz contracted scale in  $z$ -direction.

The maximal energy density in the p-Pb reaction (at  $t = 0.002$  fm/c) is comparable with that in heavy-ion collisions at the LHC energy for local cells due to fluctuations of the initial conditions in PHSD (in case of a high spatial resolution). Note that the formed high energy density "tube" is strongly Lorentz contracted along the collision axis  $z$  and is reminiscent of the energy density in a 'string' that stretches in the longitudinal direction with increasing time.

### 3.2. Charged particle multiplicities and their distributions

With the elementary p-p collisions in the PHSD being adjusted at LHC energies via PYTHIA 6.4 (using the Innsbruck pp tune (390)) we now proceed with observables and correlations from p-Pb collisions. In Fig. 3(a) we present the probability distribution in the participant number  $N_{part}$  and the number of charged hadrons at midrapidity  $N_{ch}(\eta = 0)$  as well as the different projections for p-Pb (5.02 TeV) in (b) and (c). In this figure it was assumed that the charged particles are distributed according to negative binomial distributions in the Glauber calculation. As is seen from Fig. 3, the number of charged particles at midrapidity correlates with the number of participants,  $N_{ch}(\eta = 0) \sim N_{part}$ , however, with a large dispersion in both quantities. If this 2D distribution is integrated over the number of charged particles, the  $P(N_{part})$  distributions for various models are compared in Fig. 3(b) and 3(c). For  $N_{part} \gtrsim 15$ , the Gribov-Glauber (GG) distributions (calculated in the WNM) (full squares and triangles in

(b)) increasingly overshoot the standard Glauber (G) result (full dots in (b))<sup>‡</sup> and this difference reaches an order of magnitude in the case of  $N_{part} \gtrsim 30$  while all evaluated distributions practically coincide for low numbers of participants,  $N_{part} \lesssim 15$ . In contrast to the Glauber or Gribov-Glauber Monte Carlo simulations we find no dramatic enhancement in the distribution when taking into account the cross section fluctuations in the PHSD (PHSD-GG, red dotted line compared to the blue solid line); the  $P(N_{part})$  distribution is close to the Glauber-Gribov results in PHSD (Fig. 3(b)). The noted difference is seen in the correlation  $N_{ch}/d\eta(\eta=0)$  vs.  $N_{part}$ . Both the standard Glauber and CGC results are presented and support the results of Ref. [39]. However, the two versions of the PHSD model, with (red dotted line) and without cross section fluctuations (blue solid line), predict that the multiplicity dependence turns out to be close to the

<sup>‡</sup> In contrast to the PHSD-GG case, for the Glauber calculations we use the constant parameter  $\Omega = 0.55$  or  $\Omega = 1.01$  to enhance the influence of cross section fluctuations.

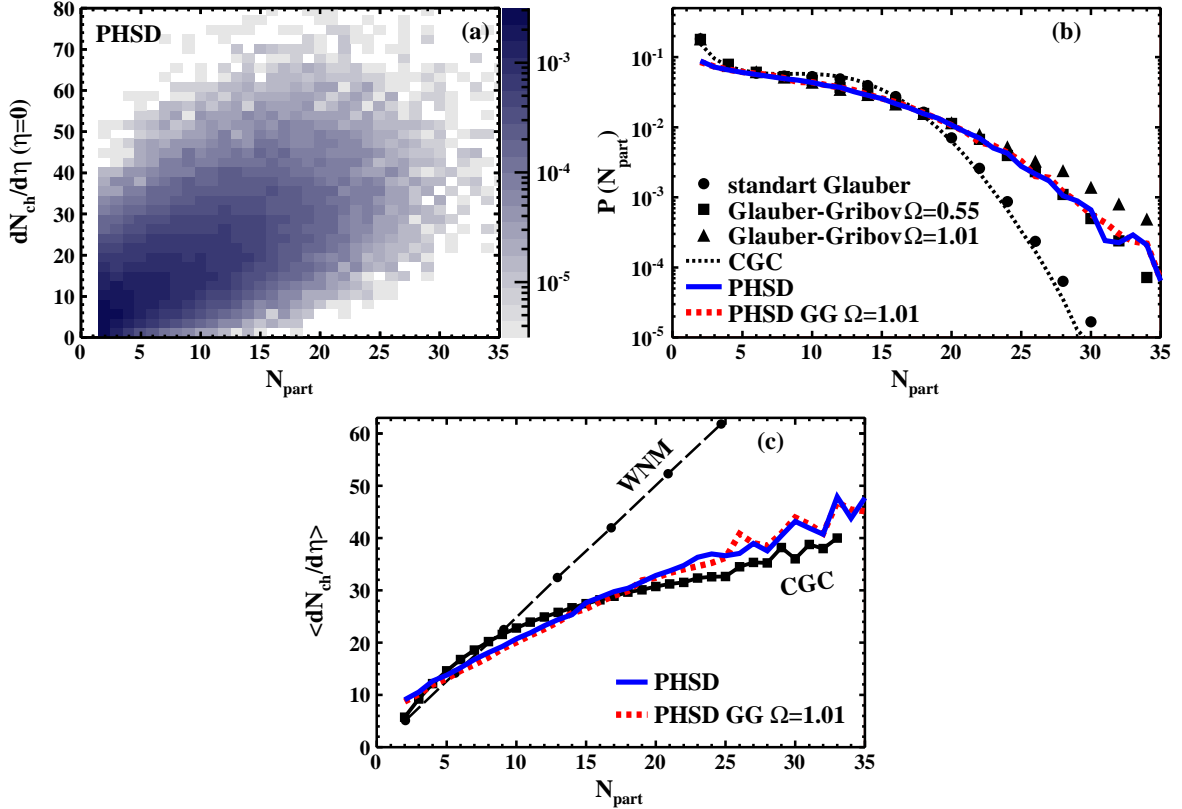


**Figure 3.** Probability distribution of the participant number and number of charged particles for p-Pb at  $\sqrt{s_{NN}} = 5.02$  TeV at midrapidity (a) and its different projections in (b) and (c). The wounded nucleon model (WNM)(full dots -standart Glauber) and color glass condensate (CGC) calculations (dotted line in (b)) are taken from [39] while simulations in the Glauber-Gribov approximation (full squares and triangles) stem from [55]. The PHSD results are displayed in terms of the solid (blue) lines while the PHSD results including fluctuations in the cross section are shown in terms of the dotted (red) lines.



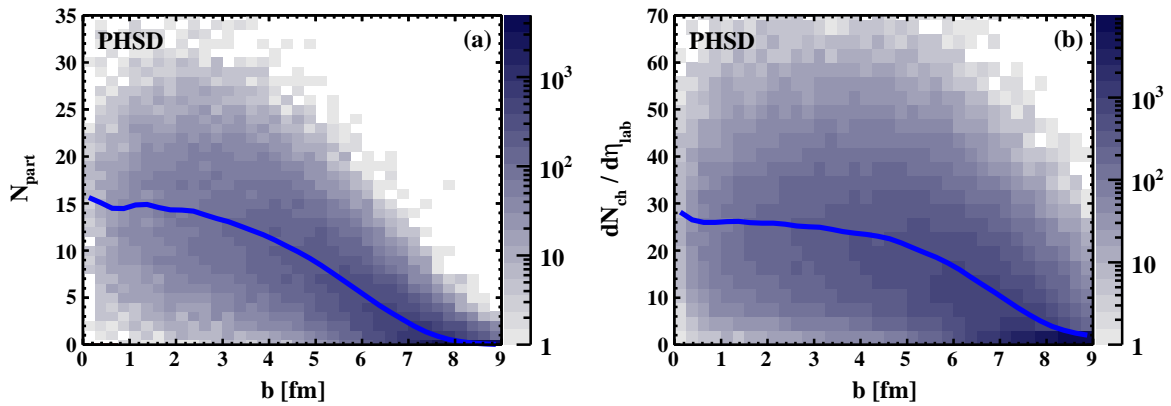


**Figure 4.** Event distributions of 2D-correlations for the participant number  $N_{part}$  (a) and charged particle multiplicity  $dN_{ch}/d\eta$  (b) with the impact parameter  $b$ . The mean values of these distributions are shown by the solid (blue) lines.

CGC result and is only weakly sensitive to the parameter  $\Omega$  for the size of the fluctuations in the cross section. Thus, multiplicity distributions do not allow us to disentangle the different initial states under discussion. The reason of such a multiplicity suppression is the energy-momentum conservation in PHSD which on average results in a decrease of particle multiplicity in subsequent scatterings as compared to the primary interaction. This is directly confirmed by a degradation of the energy density distribution in the longitudinal direction in Fig. 2(b).

A wide distribution is also observed in the number of participants or in the number of charged particles at midrapidity for a given impact parameter  $b$ , see Fig. 4. The solid lines in this figure show the mean values  $\langle N_{part} \rangle$  and  $\langle dN_{ch}/d\eta \rangle$ , respectively. In contrast to nucleus-nucleus collisions, these mean quantities are almost independent of the impact parameter for central and semi-central collisions,  $b \lesssim (4-5)$  fm. This fact should have been expected since the size of the projectile-proton is noticeably smaller than that of the target nucleus. From these results it follows that an event selection with respect to the number of participants or charged particles refers to a large range in impact parameter.

### 3.3. Rapidity distribution

The pseudorapidity distributions of charged particles from p-Pb minimum bias collisions at  $\sqrt{s_{NN}} = 5.02$  TeV are compared with the experimental data [32] in Fig. 5. The data are displayed in the laboratory system which is shifted with respect to the nucleon-nucleon center-of-mass by  $y_{cm} = -0.465$ . The results of two versions of the parton-hadron string dynamics model (PHSD and PHSD-GG) differ only for backward-emitted particles and both versions are rather close to the measured data and the CGC result (open circles). Note that there are no modifications (or free parameters) in the PHSD except the extensions pointed out in Sec. II which implies that p-p, p-A and A-A collisions are consistently described from low SPS to LHC energies (within  $\sim 10\%$ ).

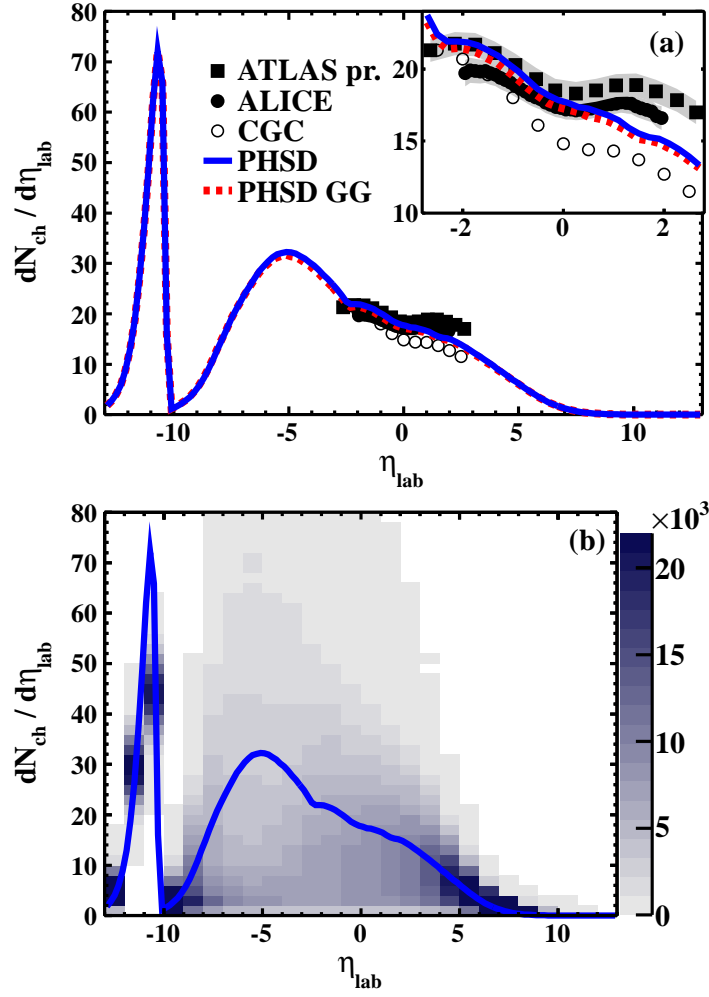


**Figure 5.** (a) Rapidity distribution of charged particles for minimum bias data from the ALICE [32] (full dots) and ATLAS [55] (full squares) collaborations for p-Pb collisions at  $\sqrt{s_{NN}} = 5.02$  TeV in comparison to the PHSD results (solid blue line) and the PHSD GG results including fluctuations in the cross section (dotted red line). The CGC results (open circles) have been taken from Ref. [35]. The zoomed results are displayed in the insertion. (b) Event-by-event fluctuations of the rapidity distribution. The blue solid line shows the average charged particle pseudorapidity distribution.

The CGC predictions, performed earlier for the upcoming p-Pb run at the LHC, are plotted in the same figure [35] (open circles). This result is based on the Balitsky-Kovchegov (BK) equation [54] which is the large- $N_c$  limit of non-linear renormalization group equations such as the (outlined-above) BK-JIMWLK hierarchy [27] tested with respect to  $e + p$  data. The inclusion of running coupling corrections to the evolution kernel of the BK equation (rcBK model) made it possible to describe various data at high energies in terms of solutions of the rcBK equation [56] and turned out in the best agreement among the compilation of CGC saturated models in Ref. [35]. An astonishing result is that the CGC and PHSD results almost coincide again. Note that this minimum-bias distribution corresponds to the mean charged particle multiplicity

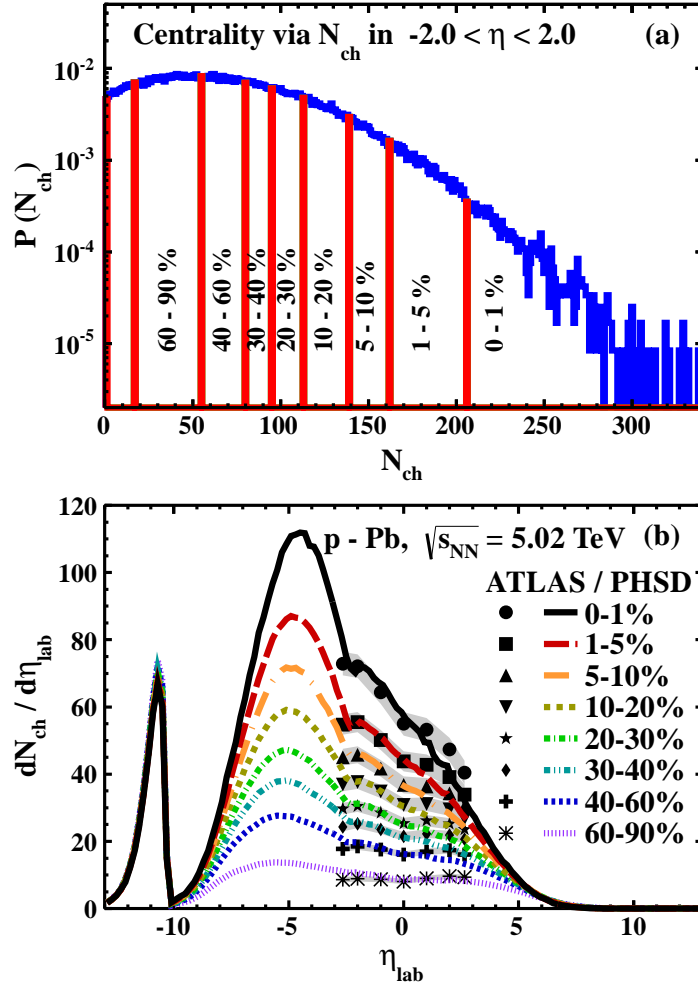


**Figure 6.** (a) Centrality bins for p-Pb collisions at  $\sqrt{s_{NN}} = 5.02$  TeV selected according to the charged particle multiplicity in the rapidity interval  $|\eta| < 2$ . (b) Comparison of the PHSD calculated rapidity distributions with ATLAS data [55] for charged particles in different centrality bins. The shaded bands show the experimental uncertainties.

at the given value of pseudorapidity  $\eta$ . However, event fluctuations of  $dN_{ch}/d\eta$  are very large as demonstrated in Fig. 5(b). Thus, the study of minimum-bias  $dN_{ch}/d\eta$  does not allow to disentangle the initial state concepts described within the PHSD and CGC approaches.

Let us, furthermore, consider pseudorapidity distributions for fixed high-multiplicity events. Such distributions for different centrality bins have been measured recently by the ATLAS collaboration [55] for p-Pb collisions at  $\sqrt{s_{NN}} = 5.02$  TeV. Experimentally the centrality was defined according to selected bins in the transverse energy. We have defined corresponding bins in  $N_{ch}$  keeping the same percentage of the number of selected events as in [55] (the bin partition is shown in Fig. 6(a) and the relative contribution of different centralities is given in the legend in Fig. 6(b)). In this figure the PHSD results are based on  $10^6$  simulated events.

As is seen from Fig. 6(b), the PHSD model quite well reproduces the shape of the  $dN_{ch}/d\eta$  distributions and its variation with centrality, in particular the increase with centrality of the forward-backward asymmetry between the directions of the proton-beam and Pb-target. For the most central events the PHSD calculations very slightly overshoot this asymmetry, however, are in line with the data for the higher centralities within the experimental uncertainties (shaded areas in Fig. 6(b)). We mention that the centrality sample of 40-60% with the maximal number  $N_{ch} \sim 20$  roughly corresponds to the minimum-bias distribution. For events of the highest multiplicity which amount to (0-1)% – corresponding to  $\sim 6.10^3$  simulated events – the number of charged particles at the maximum of the distribution is about 75. The agreement between calculations and data is not so bad taking into account the experimental error bands and the fact that PHSD has no free parameters once the p-p dynamics is fixed (by the PYTHIA tune). This holds for p-A as well as A-A reactions in a wide energy regime and for all centrality classes.

### 3.4. Transverse momentum spectra

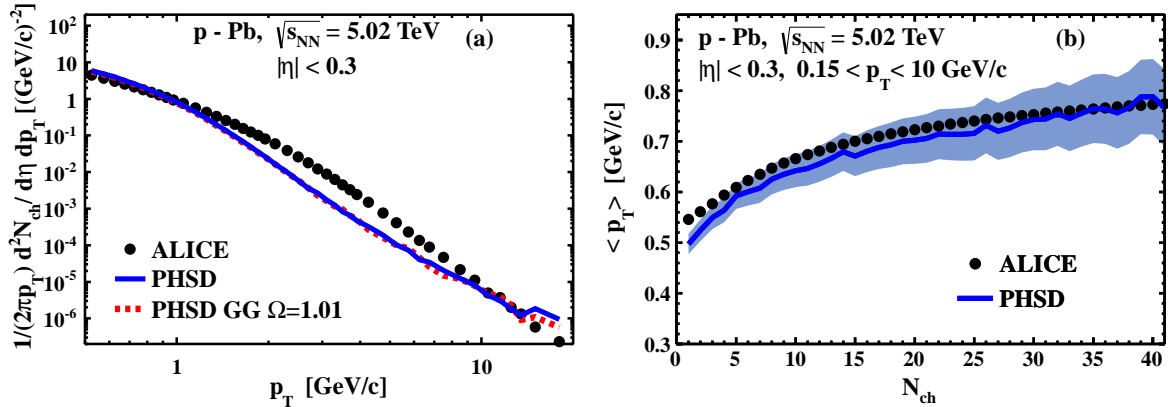


**Figure 7.** (a) Transverse momentum spectrum at midrapidity and (b) the mean transverse momentum vs. charged particle multiplicity for p-Pb collisions at  $\sqrt{s_{NN}} = 5.02$  TeV in comparison to the ALICE data [57, 58]. The shaded area in (b) shows the statistical uncertainty of the PHSD calculations.

The transverse momentum characteristics for charged particles from the PHSD for p-Pb collisions at  $\sqrt{s_{NN}} = 5.02$  TeV are compared with the ALICE data in Fig. 7. In the measured range  $0.5 < p_T < 10$   $\text{GeV}/c$  the yield changes by 7 orders of magnitude in a rough agreement with experiment [57]. Deviations by up to a factor of three are observed in the momentum range  $p_T \gtrsim 1.5$   $\text{GeV}/c$  (see Fig. 7(a)) and are presently not understood. Nevertheless, the dependence of the mean transverse momentum  $\langle p_T \rangle$  on the number of charged particles (Fig. 7(b)) is rather well described which implies that the 'soft' physics is sufficiently under control in PHSD. In view of Fig. 1(d) this result is basically due to the specific PYTHIA 6.4 tune (390) that rather well reproduces this correlation for p-p collisions at 7 TeV. We note in passing that various PYTHIA tunes

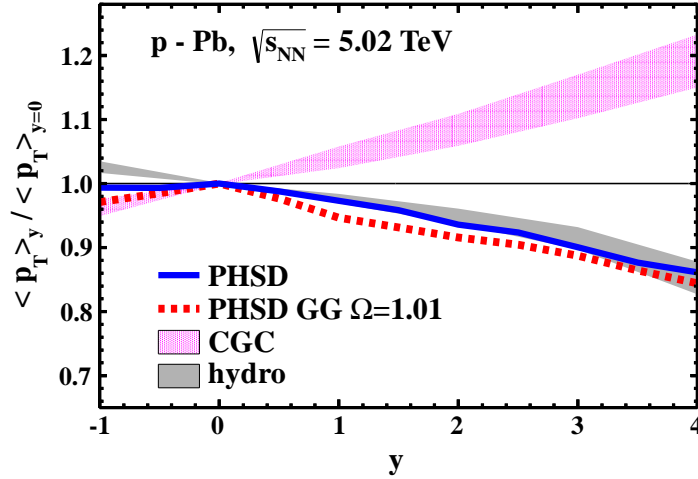


**Figure 8.** The average relative transverse momentum of produced charged particles as a function of rapidity for p-Pb collisions at  $\sqrt{s_{NN}} = 5.02$  TeV. The solid (blue) line is the default PHSD prediction whereas the dotted (red) line shows the result including large fluctuations in the initial cross section. The CGC and hydrodynamic results are taken from Ref. [40]. The shaded areas correspond to the uncertainty in two selected CGC models and in the centrality selection in the hydro case, respectively.

used before by some experimental collaborations fail in reproducing this correlation. Additionally, there is practically no sensitivity to fluctuations in the initial  $NN$  cross sections when using the PHSD-GG version.

A remarkable difference in observables between the predictions of the saturated CGC and hydro models has been pointed out in Ref. [40]. Based on general arguments, it was shown that in the case of the CGC the mean transverse momentum slightly grows with increasing rapidity  $y$  on the proton side due to the increasing saturation momentum  $Q_s$  of the nucleus (see Fig. 8). On the contrary, the  $\langle p_T \rangle_y / \langle p_T \rangle_{y=0}$  in the hydrodynamical framework (with Glauber initial conditions) decreases due to the decreasing number of particles with positive rapidity. This is due to the fact that the collective expansion scenario (in hydrodynamics) cannot lead in a simple way to an increase of the average transverse momentum on the proton side  $y > 0$  [40] since there are less degrees of freedom to generate e.g. a transverse flow. The PHSD model predicts the  $\langle p_T \rangle$  distribution (blue solid line) to be rather close to the hydrodynamic models since also in PHSD the collectivity is correlated with the density of degrees of freedom which decreases with forward rapidity (cf. Fig. 5); cross section fluctuations have no essential influence on this result (dotted red line). It would be of great interest to check experimentally this clear difference in the  $\langle p_T \rangle_y / \langle p_T \rangle_{y=0}$  distribution due to different initial state concepts.

## 4. Conclusions

In this study the parton-hadron-string dynamics (PHSD) approach has been extended to the LHC energy range by implementing additionally the PYTHIA 6.4 generator (employing the Innsbruck pp tune (390)) to describe adequately initial hadron interactions in the TeV energy range (cf. Fig. 1) and to take into account additionally fluctuations of nucleon-nucleon cross sections (in the sense of the 'Glauber-Gribov' model). The PHSD approach quite reasonably reproduces observables of p-Pb collisions at  $\sqrt{s_{NN}} = 5.02$  TeV, including those for high multiplicity events, also with respect to the pseudorapidity dependence. The calculated PHSD results have been confronted with predictions from saturation CGC models in order to disentangle the inherent assumptions with respect to the initial state conditions and dynamics.

We have found that the test for color coherence in the initial state in ultrarelativistic p-Pb collisions (as proposed in [39]) turned out to be not conclusive. This proposal had been based on wounded-nucleon model (WNM) estimates of the fraction of high multiplicity events. However, the WNM does not take into account the energy-momentum conservation and therefore overestimated this fraction. Our results within the dynamical PHSD calculations are only slightly above the CGC predictions and Glauber-Gribov cross section fluctuations practically do not influence the observables investigated. Accordingly, the considered quantities, – multiplicity, average transverse momentum, their distributions and correlations, – do not allow for a firm conclusion on the presence (or absence) of a color glass condensate in a Pb-nucleus at 5.02 TeV.

However, we have found that it is more promising to measure the  $\langle p_T \rangle_y / \langle p_T \rangle_{y=0}$  distribution (suggested in [40]) to obtain a more conclusive result since our PHSD calculations provide results very close to hydro calculations with a slope opposite to the CGC models. The physics behind can be expressed in simple terms: in hydro calculations as well as in PHSD the density of 'particles' decreases with rapidity on the proton rapidity side while the saturation momentum  $Q_s$  in the CGC increases with  $y$ . According experimental studies at the LHC appear feasible and should allow for a clarification.

## Acknowledgments

The authors are thankful to Adam Bzdak and Vladimir Skokov for illuminating discussions. This work in part was supported by the LOEWE center HIC for FAIR as well as by BMBF. V. D. was also partly supported by the Heisenberg-Landau grant of JINR.

## References

- [1] The results of first three years of operation of RHIC are reported in: The BRAHMS collaboration, Nucl. Phys. **A 757**, 1 (2005); The PHOBOS collaboration, Nucl. Phys. **A 757**, 28 (2005); The

- STAR Collaboration, Nucl. Phys. **A 757**, 101 (2005); The PHENIX Collaboration, Nucl. Phys. **A 757**, 184 (2005).
- [2] Y. Schutz(ed.) and U. A. Wiedemann(ed.), Proceedings of the 22nd International Conference on Ultra-Relativistic Nucleus-Nucleus Collisions (Annecy, France, 23-28 May 2011) J. Phys. G: Nucl. Part. Phys. **38**, 120301 (2011).
- [3] P. Huovinen *et al.*, Phys. Lett. B **503**, 58 (2001).
- [4] P. F. Kolb, P. Huovinen, U. Heinz, and H. Heiselberg, Phys. Lett. B **500**, 232 (2001).
- [5] D. Teaney, J. Lauret, and E. V. Shuryak, Phys. Rev. Lett. **86**, 4783 (2001).
- [6] T. Hirano and K. Tsuda, Phys. Rev. C **66**, 054905 (2002).
- [7] P. F. Kolb and R. Rapp, Phys. Rev. C **67**, 044903 (2003).
- [8] P. Huovinen, in *Quark-Gluon Plasma 3*, edited by R. C. Hwa and X.-N. Wang (World Scientific, Singapore, 2004); P. F. Kolb and U. W. Heinz, edited by R. C. Hwa and X.-N. Wang (World Scientific, Singapore, 2004).
- [9] P. Romatschke, U. Romatschke, Phys. Rev. Lett. **99**, 172301 (2007).
- [10] H. Song and U. W. Heinz, Phys. Rev. C **77**, 064901 (2008).
- [11] M. Luzum and P. Romatschke, Phys. Rev. C **78**, 034915 (2008).
- [12] B. Schenke, S. Jeon, and C. Gale, Phys. Rev. C **82**, 014903 (2010).
- [13] K. Geiger and B. Müller, Nucl. Phys B **369**, 600 (1992).
- [14] D. Molnar and M. Gyulassy, Phys. Rev. C **62**, 054907 (2000).
- [15] S. Bass, B. Müller, and D. Srivastava, Phys. Lett. B **551**, 277 (2003).
- [16] S. Plumari, A. Puglisi, F. Scardina, and V. Greco, Phys. Rev. C **86**, 054902 (2012).
- [17] Z.W. Lin, C.M. Ko, B.A. Li, B. Zhang, and S. Pal, Phys. Rev. C **72**, 064901 (2005).
- [18] Z. Xu and C. Greiner, Phys. Rev. C **71**, 064901 (2005); *ibid.* **76**, 024911 (2007); *ibid.* **81**, 054901 (2010).
- [19] W. Cassing and E. L. Bratkovskaya, Nucl. Phys. **A 831**, 215 (2009); E. L. Bratkovskaya et al., *ibid.* **A 856**, 162 (2011).
- [20] C. Nonaka and S. A. Bass, Phys. Rev. **C75**, 014902 (2007)
- [21] H. Petersen and M. Bleicher, Phys. Rev. **C81**, 044906 (2010)
- [22] G.-Y. Qin, H. Petersen, S. A. Bass, and B. Müller, Phys. Rev. **C82**, 064903 (2010)
- [23] H. Song, S. A. Bass and U. Heinz, Phys. Rev. **C83**, 024912 (2011)
- [24] H. Petersen, C. Coleman-Smith, S. A. Bass, and R. Wolpert, J. Phys. **G38**, 045102 (2011)
- [25] H. Petersen, V. Bhattacharya, S. A. Bass, and C. Greiner, Phys. Rev. **C84**, 054908 (2011)
- [26] H. Petersen, R. La Placa, and S. A. Bass, J. Phys. **G39**, 055102 (2012)
- [27] F. Gelis, E. Iancu, J. Jalilian-Marian, and R. Venugopalan, Ann. Rev. Nucl. Part. Science, **60** 463 (2010); E. Iancu, R. Venugopalan, in *Quark Gluon Plasma*, edited by R. Hwa, X. N. Wang (World Scientific, Singapore, 2003); H. Weigert, Prog. Part. Nucl. Phys. **55**, 461 (2005).
- [28] B. Schenke, P. Tribedy, and R. Venugopalan, Phys. Rev. **C 86**, 034908 (2012).
- [29] K. Werner, I. Karpenko, T. Pierog, M. Bleicher and K. Mikhailov, Phys. Rev. **C 82**, 044904 (2010); K. Werner, B. Guiot, I. Karpenko, and T. Pierog, Phys. Rev. **C89**, 064903 (2014).
- [30] J. L. Albacete, J. Phys. G: Nucl. Part. Phys. **38**, 124006 (2011).
- [31] ATLAS Collaboration, JHEP **11**, 183 (2013).
- [32] B. Abelev *et al.* [ALICE Collaboration], Phys. Rev. Lett. **110**, 032301 (2013).
- [33] A. Dumitru, D. E. Kharzeev, E.M. Levin, and Y. Nara, Phys. Rev. **C85**, 044920 (2012).
- [34] P. Tribedy and R. Venugopalan, Phys. Lett. **B710**, 125 (2012); Erratum-*ibid.* **B718**, 1154 (2013).
- [35] J. L. Albacete, A. Dumitru, H. Fujii and Y. Nara, Nucl. Phys. **A 897**, 1 (2013).
- [36] G.G. Barnafoldi, J. Barrette, M. Gyulassy, P. Levai, and V. Topor Pop, Phys. Rev. **C85**, 024903 (2012).
- [37] R. Xu, W.-T. Deng, and X.-N. Wang, Phys. Rev. C **86**, 051901 (2012).
- [38] J. L. Albacete, N. Armesto, R. Baier, et al., Int. J. Mod. Phys. **E 22** 1330007 (2013).
- [39] A. Bzdak and V. Skokov, Phys. Rev. Lett. **111**, 182301 (2013).
- [40] P. Bozek, A. Bzdak, and V. Skokov, Phys. Lett. B **728**, 662 (2014).

- [41] S. Juchem, W. Cassing, and C. Greiner, Phys. Rev. **D 69**, 025006 (2004); Nucl. Phys. **A 743**, 92 (2004).
- [42] W. Cassing, E. Phys. J. ST **168**, 3 (2009).
- [43] V. D. Toneev, V. Voronyuk, E. L. Bratkovskaya, W. Cassing, V. P. Konchakovski and S. A. Voloshin, Phys. Rev. **C 85**, 034910. (2012).
- [44] V. P. Konchakovski, E.L. Bratkovskaya, W. Cassing, V.D. Toneev and V. Voronyuk, Phys. Rev. **C 85**, 011902 (2012); E. L. Bratkovskaya, V. Ozvenchuk, W. Cassing, V. P. Konchakovski, O. Linnyk, R. Marty, and H. Berrehrah, Astron. Nachr. **335**, 612 (2014).
- [45] O. Linnyk, W. Cassing, J. Manninen, E.L. Bratkovskaya and C.M. Ko, Phys. Rev. **C 85**, 024910 (2012); O. Linnyk, E.L. Bratkovskaya, V. Ozvenchuk, W. Cassing and C.M. Ko, *ibid* **84**, 054917 (2011); O. Linnyk, W. Cassing, J. Manninen, E.L. Bratkovskaya, P.B. Gossiaux, J. Aichelin, T. Song and C.M. Ko, *ibid* **87**, 014905 (2013).
- [46] T. Sjostrand, S. Mrenna and P. Z. Skands, JHEP **0605**, 026 (2006).
- [47] H.-U. Bengtsson and T. Sjöstrand, Comp. Phys. Commun. **46**, 43 (1987).
- [48] G. Aad *et al.* [ATLAS Collaboration], New J. Phys. **13**, 053033 (2011).
- [49] E. Retinskaya, M. Luzum and J.-Y. Ollitrault, arXiv: 1401.3241.
- [50] V. Gribov, Sov. Phys. JETP **29** (1969) 483.
- [51] H. Heiselberg, G. Baym, B. Blättel, L.L. Frankfurt, and M. Strikman, Phys. Rev. Lett. **67**, 2946 (1991); B. Blättel, G. Baym, L.L. Frankfurt, H. Heiselberg, M. Strikman, Phys. Rev. **D47**, 2761 (1993).
- [52] V. Guzey and M. Strikman, Phys. Lett. **B633**, 245 (2006); Erratum in Phys. Lett. **B 663**, 456 (2008).
- [53] M. Alvioli and M. Strikman, Phys. Lett. **B722**, 347 (2013).
- [54] I. Balitsky, Nucl. Phys. **B463**, 99 (1996); Y. V. Kovchegov, Phys. Rev. **D60**, 034008 (1999).
- [55] The ATLAS collaboration, ATLAS-CONF-2013-096.
- [56] J. L. Albacete, Y. V. Kovchegov, Phys. Rev. **D75**, 125021 (2007).
- [57] B. Abelev *et al.* [ALICE Collaboration], Phys. Rev. Lett. **110**, 082302 (2013).
- [58] B. B. Abelev *et al.* [ALICE Collaboration], Phys. Lett. B **727**, 371 (2013).